

# Comparative Study of Flood Coincidence Risk in The Mainstream and Its Tributaries

**Na Li**

Wuhan University

**Shenglian Guo** (✉ [slguo@whu.edu.cn](mailto:slguo@whu.edu.cn))

Wuhan University

**Feng Xiong**

Wuhan University

**Jun Wang**

Wuhan University

---

## Research Article

**Keywords:** Flood coincidence, Copula function, Conditional probability, Comparative study, Fuhe River

**Posted Date:** June 25th, 2021

**DOI:** <https://doi.org/10.21203/rs.3.rs-644829/v1>

**License:** © ⓘ This work is licensed under a Creative Commons Attribution 4.0 International License.

[Read Full License](#)

---

1 **Comparative study of flood coincidence risk in the**  
2 **mainstream and its tributaries**

3 **Na Li, Shenglian Guo<sup>\*</sup>, Feng Xiong and Jun Wang**

4 State Key Laboratory of Water Resources and Hydropower Engineering Science, Wuhan University, Wuhan  
5 430072, China

6 <sup>\*</sup>[slguo@whu.edu.cn](mailto:slguo@whu.edu.cn)

7  
8  
9  
10  
11  
12  
13  
14  
15  
16  
17  
18  
19  
20  
21  
22  
23  
24  
25  
26  
27  
28  
29  
30  
31  
32  
33  
34  
35

36 **Abstract**

37 The coincidence of floods in the mainstream and its tributaries may lead to a large flooding in the  
38 downstream confluence area, and the flood coincidence risk analysis is very important for flood prevention  
39 and disaster reduction. In this study, the multiple regression model was used to establish the functional  
40 relationship among flood magnitudes in the mainstream and its tributaries. The mixed von Mises distribution  
41 and Pearson Type III distribution were selected to fit the probability distribution of the annual maximum  
42 flood occurrence dates and magnitudes, respectively. The joint distributions of the annual maximum flood  
43 occurrence dates and magnitudes were established using copula function. Fuhe River in the Poyang Lake  
44 region was selected as a study case. The joint probability, co-occurrence probability and conditional  
45 probability of flood magnitudes were calculated and compared with the simulated results of the observed  
46 data. The results show that the selected marginal and joint distributions perform well in simulating the  
47 observed flood data. The coincidence probabilities of flood occurrence dates in the upper mainstream and  
48 its tributaries mainly occur from May to early July. Among the three coincidence probability calculation  
49 methods, the conditional probability is the most consistent with the flood coincidence risk in the mainstream  
50 and its tributaries, which is more reliable and rational in practice. The results reflect the actual flood  
51 coincidence situation in the Fuhe River basin and can provide technique support for flood control decision-  
52 making.

53 **Keywords:** Flood coincidence; Copula function; Conditional probability; Comparative study; Fuhe River

54

55

56

57

58

59

## 60 **1 Introduction**

61 Nowadays, flood problems have become more and more prominent, which account for a large part of all-  
62 natural hazards in the world (Kvočka et al. 2016). In addition to causing severe disasters to agriculture,  
63 floods can also bring loss to the industry, life and property (de Bruijn et al. 2015; Thielen et al. 2015).  
64 Affected by human activities, climate change, environmental degradation and El Niño, extreme hydrological  
65 events occur frequently worldwide (Hirabayashi et al. 2013; Alfieri et al. 2016; Zhang et al. 2016). Against  
66 this background, the frequency and intensity of floods continue to increase, and the resulting losses are also  
67 growing (Ceola et al. 2014; Daksiya et al. 2020). Generally, large floods are caused by the combination of  
68 floods in the mainstream and its tributaries (Ganguli and Reddy 2013). When floods occur simultaneously,  
69 the flood peaks and the flood volumes will superimpose into large floods, threatening the safety of the  
70 downstream river (Chen et al. 2012; Wang 2016). Therefore, it is of great significance to study the flood  
71 coincidence laws in the mainstream and its tributaries, which can not only provide a theoretical basis for the  
72 formulation of flood control and dispatching plans in the basin, but also offer a reference for the construction  
73 of flood control facilities in the downstream.

74 For the analysis of flood coincidence, the traditional method is to statistically analyze flood coincidence  
75 events occurred based on the synchronized flood data over the years, so as to calculate the corresponding  
76 coincidence probabilities. However, the traditional hydrological statistical analysis method only focuses on  
77 historical data, and cannot quantitatively estimate the coincidence probabilities and return periods of design  
78 floods at specific frequencies. As cascade reservoirs continue to be built and put into operation, flood  
79 coincidence analysis is particularly important in joint flood control and dispatching work, but the traditional  
80 method cannot provide sufficient information. In fact, the essence of flood coincidence is a multivariable  
81 frequency combination event, which can be studied by the multivariable hydrological analysis method (Feng  
82 et al. 2020). At present, the commonly used multivariate hydrological analysis methods include the  
83 nonparametric method (Silverman 1986; Kim et al. 2006), the specific joint distribution method (Bacchi et  
84 al. 1994; Yue 2000a, 2002; Escalante 2007; Shimizu 2010), the multivariate Normal distribution method

85 (Goel et al. 1998; Yue 2000b; Prohaska and Ilic 2010), the FEI method of transforming the multi-  
86 dimensional joint distribution into one-dimensional distribution, and the empirical frequency method.  
87 However, the above methods have certain limitations and deficiencies. For example, the nonparametric  
88 method cannot give an analytical formula for the marginal distribution of variables, and the data prediction  
89 ability is weak. The specific joint distribution method requires the marginal distributions to be the same type  
90 (Shiau 2006). The multivariate Normal distribution method is prone to cause information distortion in the  
91 process of data conversion (Correia 1978). And the empirical frequency method does not have the ability to  
92 predict data extension.

93 Copula functions overcome the shortcomings of the traditional methods, and can connect arbitrary  
94 marginal distributions through correlation structures. As an effective method of constructing multivariate  
95 joint distribution, the advantages of copula functions are: (1) arbitrary marginal distribution types, (2)  
96 flexible and diverse structures, (3) simple solution method, (4) strong applicability and wide scalability. In  
97 recent years, copula functions have become a research hotspot in the field of hydrology, and been widely  
98 used in multivariate hydrological analysis. For example, they have been used for flood frequency analysis  
99 (Salvadori and Michele 2004; Zhang and Singh 2006; Reddy and Ganguli 2012; Li et al. 2013; Sraj et al.  
100 2015; Zhong et al. 2018; Karahacane et al. 2020), rainfall frequency analysis (De Michele and Salvadori  
101 2003; Kao and Govindaraju 2007, 2008; Ashkar and Aucoin 2011; Zhang and Singh 2012), rain and flood  
102 analysis (Xiao et al. 2009; Keef et al. 2009; Candela et al. 2014), and multivariate simulation (Aghakouchak  
103 et al. 2010a, b; Chen et al. 2015, 2016; Poduje and Haberlandt 2017).

104 Copula functions have also been applied in flood coincidence analysis. For example, Favre et al. (2004)  
105 used a copula function to construct the joint distribution of floods in a mainstream and its tributary, and  
106 calculated the flood coincidence probability. Wang et al. (2009) presented a Copula-based Flood Frequency  
107 (COFF) model with arbitrary marginal distributions to evaluate quantitatively flood risk at confluences.  
108 Klein et al. (2010) estimated coincidence probability of flood volumes at two reservoirs in a river basin

109 using copula functions. Schulte and Schumann (2016) developed multivariate copula-approaches to analyze  
110 coincidence risk of flood peaks in adjoining catchment. Using Copula Monte Carlo (CMC) method, Peng  
111 et al. (2017) further estimated flood risk in the confluence flood control downstream of a reservoir. However,  
112 these researches only considered flood magnitudes and ignored flood occurrence time. In fact, flood  
113 coincidence means that the simultaneous occurrence of large floods in different rivers. It needs to meet two  
114 conditions: the flood occurrence time should be within a certain range, and the flood magnitudes should be  
115 above a certain level. Therefore, when analyzing flood coincidence risk, both factors of flood occurrence  
116 time and magnitudes should be taken into consideration. Recently, assuming that the flood occurrence dates  
117 and magnitudes were independent, Chen et al. (2012) selected the multi-dimensional asymmetric  
118 Archimedean copula functions to analyze the flood coincidence risk of the upstream Yangtze River and its  
119 tributaries. Peng et al. (2019) employed multivariate copulas to estimate flood coincidence probabilities,  
120 considering flood occurrence dates and magnitudes simultaneously. Huang et al. (2018) took flood  
121 magnitudes of two rivers and flood occurrence interval dates as three reference variables, and further  
122 explored the flood hydrograph coincidence risk using copulas.

123 The above researches revealed the characteristics of flood coincidence risk from different angles, and  
124 have made great progress in the flood coincidence analysis of mainstream and its tributaries. However, some  
125 researches only focused on the coincidence risk of flood magnitudes and neglected the flood occurrence  
126 time; other researches usually assumed that the flood magnitudes and occurrence time data series were  
127 independent and ignored the correlation of flood variables. In addition, most studies were limited to  
128 constructing distribution models to quantitatively evaluate the flood coincidence risk, and hardly compared  
129 with the actual situations, which cannot guarantee the rationality and reliability of the analysis results.

130 The objective of this study is therefore to analyze flood coincidence risk in the mainstream and its  
131 tributaries considering the link of the up-downstream flood variables. Based on copula function, the joint  
132 distributions of flood magnitudes and occurrence dates are constructed for the flood coincidence analysis.

133 Daily flow data series at three hydrologic stations in the Fuhe River are chosen as a case study. First, the  
134 multivariate regression model is used to simulate the functional relationship among the flood variables of  
135 the mainstream and its tributaries. Second, the mixed von Mises and Pearson Type III marginal distributions  
136 are used to describe the annual maximum flood occurrence dates and flood magnitudes, respectively. Third,  
137 the coincidence probabilities of flood occurrence dates and magnitudes are estimated. Finally, the estimated  
138 and simulated flood coincidence risks are compared and assessed.

## 139 **2 Study area and data**

140 The Fuhe River, located at the east of Jiangxi Province and feeding into the Poyang Lake, was selected as a  
141 case study. Fig. 1 depicts the distributions of the mainstream and tributaries of the Fuhe River and related  
142 hydrological stations. Affected by the subtropical humid monsoon climate, there are abundant rainfall in the  
143 area (Wang et al. 2013). Floods are mostly formed by heavy rainstorms, which temporal and spatial  
144 distributions are consistent with heavy rains. And the flood season is generally from April to early July.  
145 Flood events occur frequently in the Poyang Lake area, with an average of 4 years every 5 years. Among  
146 the most recent major flood events are those of 1954, 1983, 1995, 1998, 1999 and 2010. One of the main  
147 causes of flood disasters in the Poyang Lake area is that the flow from the five main rivers is too large and  
148 the water level is too high, leading the floods to overflow the levee or break it. On the other hand, the river  
149 networks are huge and floods are prone to encounter, which add to the severity of flood damage.

150 As one of the five main rivers in the Poyang Lake water system, the Fuhe River is 348 km long and  
151 has a drainage area of 164,93 km<sup>2</sup>, which is the second largest river in Jiangxi Province. The Liaojiawan  
152 hydrological station with a control basin area of 8723 km<sup>2</sup>, and the Loujiacun hydrological station with a  
153 control basin area of 4969 km<sup>2</sup>, are located in the upper mainstream and tributary, respectively. The Lijiadu  
154 hydrological station with a catchment area of 15,812 km<sup>2</sup> is located in the down-mainstream, which accounts  
155 for more than 95% of the entire drainage area. In this study, the daily flow discharge data series of these  
156 three hydrological stations from 1953 to 2016 were collected and the annual maximum flood magnitudes

157 and corresponding occurrence dates were sampled.

158 [Insert Figure 1 about here]

### 159 3 Methodology

#### 160 3.1 Copula functions

161 Copula function is a multi-dimensional joint distribution function uniformly distributed in the domain of [0,  
162 1]. It can connect arbitrary marginal distributions through correlation structures to construct multi-  
163 dimensional joint distributions (Joe 1997; Nelsen 2006). Based on Sklar's theorem (Schweizer and Sklar  
164 1983), assuming that the marginal distribution functions of random variables  $x$  and  $y$ , are  $F_x(x)$  and  $F_y(y)$   
165 respectively, and  $F(x, y)$  is their joint distribution, then the copula function can be written as:

$$F(x, y) = C_\theta(F_x(x), F_y(y)) = C_\theta(u, v) \quad (1)$$

166 where  $C_\theta(\cdot)$  is a copula function;  $\theta$  is a parameter of the copula function to be estimated;  $u$  and  $v$  are  
167 marginal distribution functions, satisfying  $u = F_x(x) = P_x(X \leq x)$ , and  $v = F_y(y) = P_y(Y \leq y)$ .

168 Recently, the Archimedean copula functions have been widely used in hydrological frequency analysis  
169 (Grimaldi and Serinaldi 2006; Leonard et al. 2008; Guo et al. 2018; Yin et al. 2018). Among them, the  
170 Clayton copula (Clayton 1978), Gumbel-Hougaard copula (GH copula) (Hougaard 1986) and Frank copula  
171 (Frank 1979) are the most commonly used in practice. Because they just have one parameter and are easy  
172 to generate and solve. What's more, they can be used to describe hydrological variables with positive or  
173 negative correlations (Nelsen 2006). The mathematical expressions are shown below:

Clayton copula: 
$$C(u, v) = (u^{-\theta} + v^{-\theta} - 1)^{-1/\theta}; \theta \in (0, \infty) \quad (2)$$

GH copula: 
$$C(u, v) = \exp\left\{-\left[(-\ln u)^\theta + (-\ln v)^\theta\right]^{1/\theta}\right\}; \theta \in [1, \infty) \quad (3)$$



Frank copula:

$$C(u, v) = -\frac{1}{\theta} \ln \left[ 1 + \frac{(e^{-\theta u} - 1)(e^{-\theta v} - 1)}{(e^{-\theta} - 1)} \right]; \theta \in R \quad (4)$$

174 The parameter estimation methods of copula function mainly consist of the correlation index method,  
 175 the line-of-fit method and the maximum likelihood method. In this study, the correlation index method was  
 176 employed. Based on the relationship between the copula parameter  $\theta$  and the two variables' Kendall  
 177 correlation coefficient  $\tau$ , the parameters of copula functions can be estimated by following formula:

$$\tau = \begin{cases} \theta/(\theta + 2), & \text{Clayton} \\ 1 - 1/\theta, & \text{GH} \\ 1 - 4/\theta + 4D_1(\theta)/\theta, & \text{Frank} \end{cases} \quad (5)$$

178 where  $\tau$  is the Kendall correlation coefficient of two variables;  $\theta$  is a parameter of the copula function;  
 179 and  $D_1(\cdot)$  is the first-order Debye function.

### 180 3.2 Marginal distributions of flood occurrence dates and magnitudes

181 The flood occurrence dates often have the characteristics of periodicity. The von Mises distribution has a  
 182 good fitting effect for the distribution of periodic or seasonal variables with a single peak (Fisher 1993;  
 183 Mardia and Jupp 2009). In general, the annual maximum flood is affected by many factors, so its occurrence  
 184 dates series may be multi-peaked. In this situation, a mixed von Mises distribution which comprises  $m$  von  
 185 Mises distributions, can be applied to describe the probability density function of multi-peaked variables.  
 186 The probability density function of the mixed von Mises distribution can be written as:

$$f_x(x) = \sum_{i=1}^m \frac{p_i}{2\pi I_0(k_i)} \exp^{[k_i \cos(x-u_i)]}; 0 \leq x \leq 2\pi, 0 \leq u_i \leq 2\pi, k_i > 0 \quad (6)$$

187 where  $p_i$  is the coefficient of the mixing proportion;  $k_i$  is the scale parameter;  $u_i$  is the position parameter;  
 188  $I_0(k_i)$  is the 0-order modified Bessel function; and  $m$  is the order of the finite mixed von Mises distribution  
 189 ( $m=2$ ). The maximum likelihood estimate (MLE) method is frequently used to calculate the parameters in  
 190 Eq. (6) (Michael and Stanislav 2013).

191 For the annual maximum flood series, many distributions including the Pearson Type III (P3)  
 192 distribution, Log-Pearson Type III distribution, Gamma-type distribution, Generalized Extreme Value  
 193 (GEV) distribution, and Lognormal distribution can be used to describe the probability density function. In  
 194 China, the Pearson Type III distribution has been recommended by the Chinese Ministry of Water Resources  
 195 (MWR 2006) as a uniform procedure for flood frequency analysis. Therefore, assuming that the annual  
 196 maximum flood magnitudes obey the P3 distribution, and its probability density function is expressed as:

$$f_x(x) = \frac{\beta^\alpha}{\Gamma(\alpha)} (x - \delta)^{\alpha-1} \exp[-\beta(x - \delta)]; \alpha > 0, \beta > 0, \delta \leq x < \infty \quad (7)$$

197 where  $\alpha$ ,  $\beta$  and  $\delta$  are the shape, scale and position parameters of the P3 distribution, respectively; and  
 198  $\Gamma(\cdot)$  is the gamma function. The parameters of the P3 distribution can be estimated by the L-moment  
 199 method (Hosking 1990).

### 200 **3.3 Goodness-of-fit tests**

201 The evaluation of goodness-of-fit is a very important step in the process of selecting the marginal  
 202 distribution and the joint distribution. In order to judge whether the selected distribution is appropriate and  
 203 whether it can accurately reflect the actual distribution of the sample, it is necessary to perform a fitting test  
 204 and goodness evaluation. There are many methods for goodness-of-fit test in hydrological analysis, and the  
 205 commonly used Root Mean Square Error (RMSE), Kolmogorov-Smirnov (K-S) and chi-square ( $\chi^2$ ) test  
 206 methods were selected to evaluate the comprehensive performance of the distributions.

207 To test the goodness-of-fit of the marginal distributions and the joint distributions, the empirical  
 208 probabilities of the samples should be obtained first. For the univariate series, the empirical probabilities of  
 209 each flood variable generally can be obtained by the Weibull plotting position formula (Makkonen 2008),  
 210 which can be written as:

$$P_e(x_i) = \frac{i}{n+1} \quad (8)$$

211 where  $x_i$  is the observed data;  $n$  is the sample length; and  $P_e(x_i)$  is the empirical exceedance probability.

212 For the bivariate series, the empirical probabilities of joint distribution can be estimated using the  
213 Gringorten formula (Gringorten 1963), which has been widely applied in extreme flood events (Hirsch and  
214 Stedinger 1987; Yue 1999; Zhang and Singh 2007; Karmakar and Simonovic 2009; Xiong et al. 2019). The  
215 specific formula is as follows:

$$P_e(x_i, y_i) = \frac{\sum_{j=1}^n (X_j \leq x_i, Y_j \leq y_i) - 0.44}{n + 0.12} \quad (9)$$

216 where  $(x_i, y_i)$  is a combination of the observed data;  $n$  is the sample length; and  $P_e(x_i, y_i)$  is the empirical  
217 joint distribution probability.

218 The Root Mean Square Error (RMSE) is often selected to measure the difference between the  
219 theoretical probabilities of the fitted distribution and the empirical probabilities of the observed data. RMSE  
220 can effectively evaluate the performance of the fitted distributions. The smaller the RMSE value, the better  
221 the fitting effect. The RMSE value can be obtained as:

$$RMSE = \sqrt{\frac{1}{n} \sum_{i=1}^n (P_{ei} - P_i)^2} \quad (10)$$

222 where  $n$  is the sample size;  $P_i$  is the theoretical probabilities obtained from the fitted distribution;  $P_{ei}$  is the  
223 empirical frequencies from the observed data.

224 The Kolmogorov-Smirnov (K-S) test is a goodness-of-fit test method that analyzes the distance  
225 between the empirical distributions and the theoretical distributions (Massey 1951; Weiss 1978; Razali and  
226 Wah 2011). It can judge whether the observed data of the sample obey the fitted distribution. For  $n$  observed  
227 data which are in an increasing order, the K-S test statistic is expressed as:

$$D_n = \sup_x |F_n(x) - F^*(x)| \quad (11)$$

228 where  $F^*(x)$  is the theoretical distribution;  $F_n(x)$  is the empirical distribution,  $\sup_x$  is the maximum

229 value of distances.

230 The chi-square ( $\chi^2$ ) test is to measure the degree of deviation between the observed values and the  
231 predicted values. The size of the chi-square value determines the degree of deviation. The chi-square test  
232 statistic is defined as:

$$\chi^2 = \frac{(M_1 - np_1)^2}{np_1} + \frac{(M_2 - np_2)^2}{np_2} + \dots + \frac{(M_k - np_k)^2}{np_k} \quad (12)$$

233 where  $p_1, p_2, \dots, p_k$  are the hypothesized probabilities for  $k$  possible outcomes; and  $M_1, M_2, \dots, M_k$  are the  
234 observed counts of each outcome to be compared for expected counts  $np_1, np_2, \dots, np_k$  in  $n$  independent  
235 trails.

### 236 3.4 Estimation of flood coincidence risk

237 Flood coincidence means large floods in the mainstream and its tributaries occur simultaneously. In general,  
238 the probabilities are used to quantitatively describe the degree of flood coincidence. According to the  
239 definition of flood coincidence, it is obvious that flood events are mainly characterized by flood occurrence  
240 dates and flood magnitudes. Thus, both factors should be taken into consideration when evaluating flood  
241 coincidence. In this study, the flood occurrence dates and flood magnitudes were selected as reference  
242 variables.

#### 243 3.4.1 Coincidence risk of flood occurrence dates

244 Considering flood occurrence dates, the coincidence of flood occurrence dates refers to that the annual  
245 maximum floods in the mainstream and its tributaries occur on the same day. Therefore, the coincidence  
246 probabilities of the annual maximum flood occurrence dates of two rivers on the  $k$ th day can be defined as:

$$\begin{aligned} P_k' &= P(t_k < T_i \leq t_{k+1}, t_k < T_j \leq t_{k+1}) \\ &= F_T(t_k, t_k) + F_T(t_{k+1}, t_{k+1}) - F_T(t_k, t_{k+1}) - F_T(t_{k+1}, t_k) \end{aligned} \quad (13)$$

247 where  $i$  and  $j$  are the hydrological stations on the mainstream and its tributary;  $T_i$  represents the occurrence

248 dates of the annual maximum flood, expressed as a certain day of the flood season; and  $t_k$  represents the  $k$ th  
 249 day of the flood season.

### 250 **3.4.2 Coincidence risk of flood magnitudes**

251 Considering flood magnitudes coincidence, we can establish joint distributions of the annual maximum  
 252 floods in the mainstream and its tributaries based on copula functions. Then, the flood coincidence risk can  
 253 be quantitatively evaluated using the joint probabilities, co-occurrence probabilities and conditional  
 254 probabilities.

255 For the joint probabilities of flood magnitudes coincidence, it refers to the probabilities that at least  
 256 one of two rivers occurs floods surpassing certain values, expressed as the following equation:

$$P(X > x \cup Y > y) = 1 - F(x, y) = 1 - C(u, v) \quad (14)$$

257 where  $x$  and  $y$  are the flood magnitudes in  $i$  and  $j$  river, respectively; and  $F(x, y)$  is the joint distribution  
 258 function of flood magnitudes in two rivers.

259 For the co-occurrence probabilities of flood magnitudes coincidence, it refers to the probabilities that  
 260 two rivers simultaneously occur floods surpassing certain values, expressed as the following equation:

$$\begin{aligned} P(X > x \cap Y > y) &= 1 - F_x(x) - F_y(y) + F(x, y) \\ &= 1 - u - v + C(u, v) \end{aligned} \quad (15)$$

261 For the conditional probabilities, it refers to the probabilities that when given range for any one  
 262 variable, the other variable fall into another range. In this study, under the condition that one river has  
 263 occurred floods surpassing certain values, the probability that another river also occurs floods surpassing  
 264 certain values, can be expressed as the following equation:

$$\begin{aligned} P(Y > y | X > x) &= \frac{P(X > x \cap Y > y)}{P(X > x)} \\ &= \frac{1 - F_x(x) - F_y(y) + F(x, y)}{1 - F_x(x)} = \frac{1 - u - v + C(u, v)}{1 - u} \end{aligned} \quad (16)$$

## 265 4 Results and discussion

### 266 4.1 Flood correlation analysis

267 There are many methods to measure the correlation between variables in hydrological analysis, and the  
268 common Pearson correlation coefficient was used to describe the correlation between the annual maximum  
269 flood magnitudes series of these three hydrological stations in the Fuhe River. Fig. 2(a) shows the correlation  
270 analysis of the annual maximum flood magnitudes between the Liaojiawan, Loujiacun stations in the  
271 upstream and the Lijiadu station in the downstream, respectively. It can be seen that the Pearson correlation  
272 coefficient between the Liaojiawan and Lijiadu stations is 0.93, and between the Loujiacun and Lijiadu  
273 stations is 0.90. There are strong positive correlation in the annual maximum flood magnitudes between  
274 these stations. Since the control basin area of the Loujiacun station is smaller than that of the Liaojiawan  
275 station, its correlation with the Lijiadu station is relatively small.

276 Fig. 2(b) shows the correlation analysis of the annual maximum flood magnitudes between the  
277 Liaojiawan and Loujiacun stations which are both located in the upper reaches of the Fuhe River. It can be  
278 seen that the Pearson correlation coefficient is 0.80, and their control basins are very close in space.  
279 Therefore, the key factors for flood generation, such as climatic conditions, geographical environment and  
280 topographical position, are very similar. It also proves that the regularity of flood occurrence in the upper  
281 reaches is highly consistent.

282 In order to analyze the quantitative relationship among the annual maximum flood magnitudes series  
283 of the three stations, the multiple regression model was employed. The functional relationship among the  
284 annual maximum flood magnitudes of these three stations was constructed, and the result is as follows:

$$Y = \hat{Y} + \varepsilon = 104.890 + 0.841X_1 + 1.082X_2 + \varepsilon \quad (17)$$

285 where  $X_1$  and  $X_2$  represent the observed values of the annual maximum flood magnitudes at the  
286 Liaojiawan and Loujiacun stations, respectively;  $\hat{Y}$  represents the simulated values of the annual maximum  
287 flood magnitudes at the Lijiadu station;  $\varepsilon$  is the random error of the model, obeying a Normal distribution

288 with a mean value of 0, which can be expressed as  $\varepsilon : N(0, \sigma_\varepsilon^2)$ .

289 To evaluate the performance of the multiple regression equation, the relationship between the simulated  
290 values of the annual maximum flood magnitudes obtained by the multiple regression model and the observed  
291 values at the Lijiadu station, is plotted in Fig. 3. It can be seen that the scattered points are basically  
292 distributed along the 45° diagonal, indicating the simulated values and the observed values are very close.  
293 It further proves that the floods at the Lijiadu station are mainly formed by the superposition of the upstream  
294 floods, and the simultaneous occurrence of floods in the upstream are easy to cause large flooding in the  
295 downstream confluence area.

296 [Insert Figure 2 about here]

297 [Insert Figure 3 about here]

#### 298 **4.2 Estimation of marginal distributions**

299 The mixed von Mises distribution was used to fit the occurrence dates series of the annual maximum flood  
300 at the three stations in the Fuhe River, and the parameters of the marginal distributions were estimated by  
301 the maximum likelihood method. Table 1 lists the values of the estimated parameters of the von Mises  
302 function. The empirical frequencies of the marginal distributions were obtained by Eq. (8), and the  
303 theoretical probabilities of the mixed von Mises distribution were calculated by Eq. (6). Fig. 4 shows the  
304 fitting relationship between the empirical frequency points and the theoretical probability curve for the  
305 annual maximum flood occurrence dates, in which the mixed von Mises distribution can fit the empirical  
306 distribution very well.

307 In order to evaluate the performance of the marginal distributions more comprehensively, the K-S test  
308 method was used for the fitting test, and the Root Mean Square Error method was applied for the goodness  
309 evaluation. The results of the goodness-of-fit evaluation are presented in Table 1. It is shown that at a  
310 significance level of 0.05, the values of K-S test statistics do not exceed their critical values, implying that  
311 all the marginal distributions of the annual maximum flood occurrence dates have passed the hypothesis

312 test. Meanwhile, the RMSE values between the theoretical frequencies and the empirical probabilities are  
313 small enough. Therefore, the mixed von Mises distribution performs well in simulating the annual maximum  
314 flood occurrence dates in the Fuhe River.

315 The P3 distribution was applied to describe the annual maximum flood magnitudes series of the three  
316 stations, and the parameters were estimated by the L-moment method. The values of the estimated  
317 parameters of the P3 distribution are presented in Table 2. The empirical frequencies and the theoretical  
318 probabilities were calculated by Eqs. (8) and (7), respectively. The fitting curves of the marginal  
319 distributions are shown in Fig. 4. It can be seen that graphically, the P3 distribution fits the empirical  
320 distributions well. In addition, the chi-square test and the Root Mean Square Error method were selected for  
321 the fitting test and goodness evaluation. Table 2 lists the relative evaluation index results. It is shown that  
322 the p-values of the chi-square test of the three stations are all larger than the critical values at the 0.05 level  
323 of significance, implying that the hypothesis test that the flood magnitudes obey the P3 distribution is not  
324 rejected. So, the P3 distribution performs well in quantifying the marginal distributions of the annual  
325 maximum flood magnitudes.

326 [Insert Table 1 about here]

327 [Insert Table 2 about here]

328 [Insert Figure 4 about here]

### 329 **4.3 Estimation of joint distributions**

330 The dependence of the annual maximum floods among these three stations have been verified. Thus, the  
331 copula functions can be used for the flood coincidence analysis. Based on the Clayton, GH and Frank copula  
332 functions, the bivariate joint distribution of the annual maximum flood occurrence dates at the Liaojiawan  
333 and Loujiacun stations was constructed. Similarly, the two-dimensional joint distributions of the annual  
334 maximum flood magnitudes between the Liaojiawan, Loujiacun and Lijiadu stations were also constructed,  
335 respectively. The Kendall rank correlation coefficient was employed to reckon the parameters of the



336 Archimedean copula functions. Table 3 presents the values of the estimated parameters. Using the Eq. (9),  
337 the empirical frequencies of the joint distributions were calculated. In order to select the most appropriate  
338 copula function among the three candidate copulas, the Root Mean Square Error method was applied to test  
339 the goodness of fitting. The RMSE values between the empirical frequencies and the theoretical  
340 probabilities are listed in Table 3. The results show that for the annual maximum flood occurrence dates and  
341 flood magnitudes, the RMSE values of the Clayton copula function are the lowest. It indicates that the  
342 Clayton copula function is the most appropriate copula for modeling the joint distributions of flood variables  
343 at these stations of the Fuhe River. Therefore, the Clayton copula function is selected to establish the joint  
344 probability distributions of the annual maximum flood occurrence dates and magnitudes, respectively. The  
345 theoretical and the observed nonexceedance joint probabilities are exhibited in Fig. 5, in which the x-axis is  
346 sorted in ascending order of the theoretical nonexceedance joint probabilities. It can be seen that the  
347 theoretical frequency curves can fit the observed values well.

348 [Insert Table 3 about here]

349 [Insert Figure 5 about here]

#### 350 **4.4 Analysis of flood coincidence risk**

##### 351 **4.4.1 Coincidence risk of flood occurrence dates**

352 With Eq. (13), the coincidence probabilities of the occurrence dates of the annual maximum flood at the  
353 Liaojiawan and Loujiacun stations were calculated and the results are presented in Fig. 6. The curve  
354 demonstrates that the coincidence probabilities of flood occurrence dates in the mainstream and tributaries  
355 of the upper Fuhe River present the characteristics of multiple-peak. Before March and after August, the  
356 coincidence probabilities are very small, which are basically close to zero. During the period from mid-  
357 March to late April, there are a relatively stable coincidence risk, which are almost below 0.015%. Early  
358 May to early July is a higher coincidence period of the flood occurrence dates, including two peaks. The  
359 first coincidence peak occurs on May 12, with an associated probability of 0.026%. The second peak with

360 an associated probability of 0.057% occurs on June 21, which is the largest coincidence risk. According to  
361 the analysis of climate, it can be known that the Fuhe River is located in the subtropical monsoon climate  
362 zone, and the flood season is from April to July. During this period, the precipitation is frequent and the  
363 precipitation intensity is high, which is easy to cause floods. Moreover, floods have obvious characteristics  
364 that change with the seasons. The annual flow is mainly distributed in the flood season, and most of the  
365 large floods occur in individual months of the flood season, such as May, June and July. From the beginning  
366 to the end of the flood season, the flood intensity changes from weak to strong, and then from strong to  
367 weak. Therefore, May to early July are the overlapping periods of floods in the mainstream and tributaries.  
368 As shown in Fig. 6, the higher coincidence probabilities of the occurrence dates of the annual maximum  
369 flood occur in May to early July, which proves that the calculated results are in accordance with the actual  
370 situation. Adding together all the daily coincidence probabilities of the flood occurrence dates, expressed as

371 
$$P^t = \sum_{k=1}^n P_k^t$$
, we can obtain the coincidence probability of the annual maximum flood occurrence dates in  
372 the mainstream and tributaries, and the result is 2.87%.

373 [Insert Figure 6 about here]

#### 374 4.4.2 Coincidence risk of flood magnitudes

375 The coincidence probabilities of the annual maximum flood magnitudes for different design floods in the  
376 mainstream and its tributaries were estimated. With Eqs. (14) and (15), the joint probabilities and the co-  
377 occurrence probabilities of  $T$ -year design floods at the Liaojiawan and Loujiacun stations were calculated,  
378 respectively. With Eq. (16), the conditional probabilities of the occurrence of  $T$ -year design floods at the  
379 Lijiadu station, when given the occurrence of floods at the Liaojiawan station were obtained. In the same  
380 manner, the conditional probabilities of  $T$ -year design floods occurring at the Lijiadu station, given floods  
381 at the Loujiacun station were also calculated. Tables 4 and 5 display the flood coincidence probabilities  
382 including the joint probabilities, co-occurrence probabilities, and conditional probabilities for 5, 10, 20, 50,  
383 and 100-year design floods in the Fuhe River basin.

384 It can be seen that the joint probabilities of the occurrence of 5, 10, 20, 50 and 100-year design floods  
385 at the Liaojiawan and Loujiacun stations are 30.48%, 17.14%, 9.20%, 3.86%, and 1.96%, respectively. The  
386 co-occurrence probabilities for different design floods with the return periods of 5, 10, 20, 50 and 100 years  
387 at the Liaojiawan and Loujiacun stations are 9.52%, 2.86%, 0.80%, 0.14% and 0.04%, respectively.  
388 Obviously, the joint probabilities are greater than the co-occurrence probabilities for different design floods.  
389 The results show that as the return periods increase, the joint probabilities and co-occurrence probabilities  
390 of flood magnitudes coincidence decrease. That is, small and medium floods are more likely to occur  
391 simultaneously, which conforms to the general law in practice.

392 Given the occurrence of 5, 10, 20, 50, and 100-year design floods at the Liaojiawan station, the  
393 conditional probabilities of the same flood magnitudes occurring at the Lijiadu station are 16.41%, 5.01%,  
394 1.46%, 0.26%, and 0.07%, respectively. Similarly, given the occurrence of 5, 10, 20, 50, and 100-year  
395 design floods at the Loujiacun station, the conditional probability of the same flood magnitudes occurring  
396 at the Lijiadu station are 15.21%, 4.47%, 1.26%, 0.22%, and 0.06%, respectively. It can be seen that floods  
397 with lower return periods result in higher coincidence probabilities. The conditional probabilities between  
398 the Liaojiawan and Lijiadu stations are higher than that between the Loujiacun and Lijiadu stations. With  
399 reference to the previous analysis, the drainage area controlled by the Liaojiawan station is larger than that  
400 of the Loujiacun station, the correlation of flood variables between the Liaojiawan and Lijiadu stations is  
401 stronger. Therefore, the floods at the Liaojiawan station have more significant impact on the downstream  
402 floods. From the point of view, the calculated results are reasonable.

403 [Insert Table 4 about here]

404 [Insert Table 5 about here]

#### 405 **4.5 Comparison of simulation results**

406 Fig. 2 provides the evidence that the flood variables at the Liaojiawan and Loujiacun stations are highly  
407 correlated and consistent. Therefore, when floods simultaneously occur in the upper stream, the flood

408 frequencies in the mainstream and its tributaries are more likely to be the same. In this study, assuming that  
409 floods with the same frequencies simultaneously occur at the Liaojiawan and Loujiacun stations. Then based  
410 on the constructed multiple regression model, expressed as Eq. (17), the design flood at the Lijiadu station  
411 can be obtained. Flood magnitudes obey the P3 distribution, so the corresponding design frequencies can  
412 be inferred using Eq. (7). And the return periods are calculated as well. Table 6 lists: (1) the design flood  
413 values at the Liaojiawan and Loujiacun stations under the return periods of 5, 10, 20, 50, and 100 years; (2)  
414 the simulated flood values at the Lijiadu station, which are obtained by the regression model after the same  
415 frequency floods occurring in the two upstream stations; (3) the corresponding frequencies and return  
416 periods of the simulated floods at the Lijiadu station. The results show that with the rise of flood magnitudes  
417 at the Liaojiawan and Loujiacun stations, the floods at the Lijiadu station are increasing. The flood return  
418 periods of the Lijiadu station are generally longer than those of the Liaojiawan and Loujiacun stations,  
419 especially when the return periods are larger. For example, when 10-year design floods simultaneously  
420 occur at the Liaojiawan and Loujiacun stations, an 11-year flood may occur at the Lijiadu station. However,  
421 when 100-year floods simultaneously occur at the Liaojiawan and Loujiacun stations, there may be a 137-  
422 year flood at the Lijiadu station.

423 In order to verify the rationality and feasibility of the above three flood coincidence probability  
424 calculation methods, the theoretically calculated coincidence probabilities were compared with the design  
425 frequencies of the simulated flood at the Lijiadu station. Table 7 lists five conditions under different return  
426 periods, including: (1) the design frequencies of the simulated floods at the Lijiadu station when floods with  
427 the same frequency simultaneously occurring at the Liaojiawan and Loujiacun stations, (2) the joint  
428 probabilities and the co-occurrence probabilities of the same frequency floods occurring at the Liaojiawan  
429 and Loujiacun stations, (3) the conditional probabilities of the same frequency floods occurring at the  
430 Lijiadu station, given the occurrence of  $T$ -year floods at the Liaojiawan station, named  $P_1^c$ ; (4) the  
431 conditional probabilities of the same frequency floods occurring at the Lijiadu station, given the occurrence

432 of  $T$ -year floods at the Loujiacun station, named  $P_2^c$ . Meanwhile, these five flood probabilities are plotted  
433 in Fig. 7.

434 The results show that compared with the design frequencies of the simulated flood at the Lijiadu station,  
435 the joint probabilities of floods simultaneously occurring in the upper mainstream and its tributaries are  
436 generally greater, while the co-occurrence probabilities and both conditional probabilities are less. Among  
437 the four flood coincidence probabilities, the conditional probabilities ( $P_1^c$ ) are the closest to the design  
438 frequencies of the simulated floods, especially when the return periods are low. For example, the joint  
439 probability and the co-occurrence probability of 10-year floods at the Liaojiawan and Loujiacun stations are  
440 17.14% and 2.86%, respectively. At this time, the design frequency of the simulated flood at the Lijiadu  
441 station is 9.41%. The conditional probability of a 10-year flood occurring at the Lijiadu station given a 10-  
442 year flood at the Liaojiawan station is 5.01%. The conditional probability of a 10-year flood occurring at  
443 the Lijiadu station given a 10-year flood at the Loujiacun station is 4.47%. Combined with the previous  
444 analysis, we can see that flood with the same frequency simultaneously occurring at the Liaojiawan and  
445 Loujiacun stations can lead to large floods at the Lijiadu station. The corresponding design frequencies of  
446 the simulated floods are more consistent with the conditional probabilities that the same frequency floods  
447 occurring at the Lijiadu station when given  $T$ -year floods at Liaojiawan station. In practice, the floods at the  
448 Lijiadu station are basically formed by the superposition of the floods in the upper mainstream and its  
449 tributaries. More importantly, the floods at the Liaojiawan station account for a larger proportion in that of  
450 the Lijiadu station. Therefore, the results conform to the general law.

451 [Insert Table 6 about here]

452 [Insert Table 7 about here]

453 [Insert Figure 7 about here]

## 454 **5 Conclusions**

455 Flood coincidence risk analysis plays an important role in reservoir operation and flood management. In

456 this study, the coincidence probabilities of flood magnitudes and occurrence dates in the mainstream and  
457 tributaries of the Fuhe River were estimated with copula functions. The 66-year daily flow discharge data  
458 series were considered to construct the marginal distributions of flood magnitudes and occurrence dates.  
459 Based on copula functions, the joint distributions of the annual maximum flood magnitudes and occurrence  
460 dates in the mainstream and its tributaries were established, respectively. The coincidence risk of flood  
461 occurrence dates was calculated, and the coincidence analysis by joint probabilities, co-occurrence  
462 probabilities and conditional probabilities for different flood magnitudes were compared with the simulation  
463 results. The main conclusions of this study were summarized as follows:

464 (1) There is a strong consistency and significantly correlation between the floods at the upstream and  
465 downstream with the Pearson coefficients reaching 0.90. The floods at the Lijiadu station are mainly formed  
466 by the superimposition of the upstream floods. The mixed von Mises distribution and P3 distribution  
467 perform well in quantifying the marginal distributions of occurrence dates and flood magnitudes, and the  
468 Clayton copula is the best one for simulating the joint distributions of flood variables.

469 (2) The coincidence events of the annual maximum flood occurrence dates at the Liaojiawan and  
470 Loujiacun stations mainly occur from May to early July. There are two flood coincidence peaks occurring  
471 on May 12 and June 21, which coincidence probabilities are reaching 0.026% and 0.057%, respectively.  
472 The coincidence risk of the annual maximum flood occurrence dates in the upper mainstream and its  
473 tributaries throughout a year is 2.87%.

474 (3) The joint probability and co-occurrence probability of 50-year design floods at the Liaojiawan and  
475 Loujiacun stations are 3.86% and 0.14%. If a 50-year flood occurs at the Liaojiawan or Loujiacun station,  
476 the corresponding probability of a flood with the same frequency occurring at the Lijiadu station is 0.26%  
477 or 0.22%, respectively.

478 (4) Floods with the same frequencies simultaneously occurring at the Liaojiawan and Loujiacun  
479 stations are likely to superimpose into large floods at the Lijiadu station. Among the three coincidence

480 probability calculation methods, the conditional probability is the most consistent with the flood coincidence  
481 risk in the mainstream and its tributaries, which is more reliable and rational in practice.

482 In this study, the copula-based quantitative analysis of flood coincidence risk contributes us to better  
483 understand the spatiotemporal characteristics of floods in the Fuhe River. By calculating the flood  
484 coincidence probabilities of flood magnitudes and occurrence dates, we can verify the feasibility of the  
485 calculation method of flood coincidence probability considering the connection of the mainstream and its  
486 tributaries, so as to have a comprehensive knowledge in the flood coincidence laws. The results provide a  
487 scientific basis and effective support for improving the flood control capacity and ensuring the safety of  
488 flood control targets in the Poyang Lake region.

#### 489 **Acknowledgements**

490 This study was financially supported by the National Natural Science Foundation of China (51879192) and  
491 China Three Gorges Corporation (0799254).

#### 492 **Author contributions statement**

493 Shenglian Guo proposed the study, Feng Xiong and Jun Wang conducted the experiments, Na Li analyzed  
494 the results. All authors reviewed the manuscript.

#### 495 **Competing interests**

496 The authors declare no competing interests. The corresponding author is responsible for submitting a  
497 competing interest statement on behalf of all authors of the paper.

498 **References**

- 499 Aghakouchak A, Bárdossy A, Habib E (2010a) Conditional simulation of remotely sensed rainfall data  
500 using a non-Gaussian v-transformed copula. *Adv Water Resour* 33(6): 624–634
- 501 Aghakouchak A, Bárdossy A, Habib E (2010b) Copula-based uncertainty modelling: application to  
502 multisensor precipitation estimates. *Hydrol Process* 24(15): 2111–2124
- 503 Alfieri L, Feyen L, Di Baldassarre G (2016) Increasing flood risk under climate change: a pan-European  
504 assessment of the benefits of four adaptation strategies. *Clim Change* 136: 507-521.  
505 <https://doi.org/10.1007/s10584-016-1641-1>
- 506 Ashkar F, Aucoin F (2011) A broader look at bivariate distributions applicable in hydrology. *J Hydrol* 405:  
507 451–461
- 508 Bacchi B, Becciu G, Kottegoda NT (1994) Bivariate exponential model applied to intensities and durations  
509 of extreme rainfall. *J Hydrol* 155: 225–236
- 510 Candela A, Brigandì G, Aronica GT (2014) Estimation of synthetic flood design hydrographs using a  
511 distributed rainfall–runoff model coupled with a copula-based single storm rainfall generator. *Nat*  
512 *Hazards Earth Syst Sci* 14: 1819-1833
- 513 Ceola S, Laio F, Montanari A (2014) Satellite nighttime lights reveal increasing human exposure to floods  
514 worldwide. *Geophys Res Lett* 41(20): 7184–7190. <https://doi.org/10.1002/2014GL061859>
- 515 Chen L, Singh VP, Guo SL et al (2012) Flood coincidence risk analysis using multivariate copula  
516 functions. *J Hydrol Eng* 17(6): 742–755. [https://doi.org/10.1061/\(ASCE\)HE.1943-5584.0000504](https://doi.org/10.1061/(ASCE)HE.1943-5584.0000504)
- 517 Chen L, Singh VP, Guo SL et al (2015) Copula-based method for multisite monthly and daily streamflow  
518 simulation. *J Hydrol* 528: 369–384
- 519 Chen L, Singh VP, Lu WW et al (2016) Streamflow forecast uncertainty evolution and its effect on real-  
520 time reservoir operation. *J Hydrol* 540: 712–726
- 521 Clayton DG (1978) A model for association in bivariate life tables and its application in epidemiological



522 studies of familial tendency in chronic disease incidence. *Biometrika* 65(1): 141–151.  
523 <https://doi.org/10.1093/biomet/65.1.141>

524 Correia FN (1978) *Multivariate partial duration series in flood risk analysis*. Springer, Dordrecht

525 Daksiya V, Mandapaka PV, Lo EYM (2020) Effect of climate change and urbanization on flood protection  
526 decision-making. *J Flood Risk Manag* 14: e12681. <https://doi.org/10.1111/jfr3.12681>

527 de Bruijn KM, Klijn F, van de Pas B, Slager CTJ (2015) Flood fatality hazard and flood damage hazard:  
528 combining multiple hazard characteristics into meaningful maps for spatial planning. *Nat Hazards*  
529 *Earth Syst Sci* 15: 1297-1309

530 De Michele C, Salvadori G (2003) A generalized Pareto intensity duration model of storm rainfall  
531 exploiting 2-copulas. *J Geophys Res Atmos* 108(D2): 1–11. <https://doi.org/10.1029/2002JD002534>

532 Escalante SC (2007) Application of bivariate extreme value distribution to flood frequency analysis: A  
533 case study of Northwestern Mexico. *Nat Hazards* 42: 37–46. <https://doi.org/10.1007/s11069-006-9044-7>

534

535 Favre AC, Adlouni SE, Perreault L et al (2004) Multivariate hydrological frequency analysis using  
536 copulas. *Water Resour Res* 40(1): W01101. <https://doi.org/10.1029/2003WR002456>

537 Feng Y, Shi P, Qu SM et al (2020) Nonstationary flood coincidence risk analysis using time-varying  
538 Copula functions. *Sci Rep* 10: 3395. <https://doi.org/10.1038/s41598-020-60264-3>

539 Fisher NI (1993) *Statistical analysis of circular data*. Cambridge University Press, Cambridge

540 Frank MJ (1979) On the simultaneous associativity of  $F(x,y)$  and  $x+y-F(x,y)$ . *Aequationes Math* 19(1):  
541 194–226. <https://doi.org/10.1007/BF02189866>

542 Ganguli P, Reddy MJ (2013) Probabilistic assessment of flood risks using trivariate copulas. *Theor Appl*  
543 *Climatol* 111: 341–360. <https://doi.org/10.1007/s00704-012-0664-4>

544 Goel NK, Seth SM, Chandra S (1998) Multivariate modeling of flood flows. *J Hydrol Eng* 124(2): 146-  
545 155

- 546 Grimaldi S, Serinaldi F (2006) Design hyetographs analysis with 3-copula function. *Hydrol Sci J* 51(2):  
547 223–238. <https://doi.org/10.1623/hysj.51.2.223>
- 548 Gringorten II (1963) A plotting rule for extreme probability paper. *J Geophys Res* 68(3): 813–814.  
549 <https://doi.org/10.1029/JZ068i003p00813>
- 550 Guo SL, Muhammad R, Liu ZJ et al (2018) Design flood estimation methods for cascade reservoirs based  
551 on copulas. *Water* 10(5): 560
- 552 Hirabayashi Y, Mahendran R, Koirala S et al (2013) Global flood risk under climate change. *Nat Clim*  
553 *Change* 3(9): 816–821. <https://doi.org/10.1038/nclimate1911>
- 554 Hirsch RM, Stedinger JR (1987) Plotting positions for historical floods and their precision. *Water Resour*  
555 *Res* 23(4): 715–727. <https://doi.org/10.1029/WR023i004p00715>
- 556 Hosking JRM (1990) L-moments: analysis and estimation of distributions using linear combinations of  
557 order statistics. *J R Stat Soc* 52(2): 105–124
- 558 Hougaard P (1986) A class of multivariate failure time distributions. *Biometrika* 73(3): 671–678.  
559 <https://doi.org/10.2307/2336531>
- 560 Huang KD, Chen L, Zhou JZ et al (2018) Flood hydrograph coincidence analysis for mainstream and its  
561 tributaries. *J Hydrol* 565: 341–353
- 562 Joe H (1997) *Multivariate models and dependence concepts*. Chapman & Hall, London
- 563 Kao SC, Govindaraju RS (2007) A bivariate frequency analysis of extreme rainfall with implications for  
564 design. *J Geophys Res Atmos* 112(D1): 13119
- 565 Kao SC, Govindaraju RS (2008) Trivariate statistical analysis of extreme rainfall events via the Plackett  
566 family of copulas. *Water Resour Res* 44(2): W02415. <https://doi.org/10.1029/2007WR006261>
- 567 Karahacane H, Meddi M, Chebana F, Saaed HA (2020) Complete multivariate flood frequency analysis,  
568 applied to northern Algeria. *J Flood Risk Manag* 13: e12619
- 569 Karmakar S, Simonovic SP (2009) Bivariate flood frequency analysis. Part 2: a copula-based approach

570 with mixed marginal distributions. *J Flood Risk Manag* 2(1): 32-44. <https://doi.org/10.1111/j.1753->  
571 [318X.2009.01020.x](https://doi.org/10.1111/j.1753-318X.2009.01020.x)

572 Keef C, Svensson C, Tawn JA (2009) Spatial dependence in extreme river flows and precipitation for  
573 Great Britain. *J Hydrol* 378(3–4): 240–252. <https://doi.org/10.1016/j.jhydrol.2009.09.026>

574 Kim T, Valdés JB, Yoo C (2006) Nonparametric approach for bivariate drought characterization using  
575 Palmer drought index. *J Hydrol Eng* 11(2): 134-143. [https://doi.org/10.1061/\(ASCE\)1084-](https://doi.org/10.1061/(ASCE)1084-)  
576 [0699\(2006\)11:2\(134\)](https://doi.org/10.1061/(ASCE)1084-0699(2006)11:2(134))

577 Klein B, Pahlow M, Hundedcha Y, Schumann A (2010) Probability analysis of hydrological loads for the  
578 design of flood control systems using copulas. *J Hydrol Eng* 15(5): 360–369

579 Kvočka D, Falconer RA, Bray M (2016) Flood hazard assessment for extreme flood events. *Nat Hazards*  
580 84(3): 1569-1599

581 Leonard M, Metcalfe A, Lambert M (2008) Frequency analysis of rainfall and streamflow extremes  
582 accounting for seasonal and climatic partitions. *J Hydrol* 348(1–2): 135–147

583 Li TY, Guo SL, Chen L, Guo JL (2013) Bivariate flood frequency analysis with historical information  
584 based on copula. *J Hydrol Eng* 18(8): 1018–1030. [https://doi.org/10.1061/ \(ASCE\)HE.1943-](https://doi.org/10.1061/(ASCE)HE.1943-)  
585 [5584.0000684](https://doi.org/10.1061/(ASCE)HE.1943-5584.0000684)

586 Makkonen L (2008) Bringing closure to the plotting position controversy. *Commun Stat-Theory M* 37(3):  
587 460–467

588 Mardia K V, Jupp PE (2009) *Directional statistics*. Wiley, New York

589 Massey FJ (1951) The Kolmogorov–Smirnov test for goodness of fit. *J Am Stat Assoc* 46(253): 68–78

590 Michael Z, Stanislav U (2013) *Statistical decision problems*. Springer, New York

591 MWR (Ministry of Water Resources) (2006) *Regulation for Calculating Design Flood of Water Resources*  
592 *and Hydropower Projects*. Chinese Shuili Shuidian Press, Beijing (in Chinese)

593 Nelsen RB (2006) *An introduction to copulas*, 2nd edn. Springer, New York

- 594 Peng Y, Chen K, Yan HX, Yu XL (2017) Improving flood-risk analysis for confluence flooding control  
595 downstream using Copula Monte Carlo method. *J Hydrol Eng* 22(8): 04017018.  
596 [https://doi.org/10.1061/\(ASCE\)HE.1943-5584.0001526](https://doi.org/10.1061/(ASCE)HE.1943-5584.0001526)
- 597 Peng Y, Shi YL, Yan HX, Chen K (2019) Coincidence risk analysis of floods using multivariate Copulas:  
598 case study of Jinsha River and Min River, China. *J Hydrol Eng* 24(2): 05018030.  
599 [https://doi.org/10.1061/\(ASCE\)HE.1943-5584.0001744](https://doi.org/10.1061/(ASCE)HE.1943-5584.0001744)
- 600 Poduje ACC, Haberlandt U (2017) Short time step continuous rainfall modeling and simulation of extreme  
601 events. *J Hydrol* 552: 182–197
- 602 Prohaska S, Ilic A (2010) Coincidence of flood flow of the Danube River and its tributaries: Hydrological  
603 processes of the Danube River Basin. Springer, Dordrecht
- 604 Razali NM, Wah YB (2011) Power comparisons of Shapiro-Wilk, Kolmogorov-Smirnov, Lilliefors and  
605 Anderson-Darling tests. *J Stat Model Anal* 2(1): 21–33
- 606 Reddy MJ, Ganguli P (2012) Bivariate flood frequency analysis of Upper Godavari River flows using  
607 Archimedean copulas. *Water Resour Manag* 26(14): 3995–4018
- 608 Salvadori G, Michele CD (2004) Frequency analysis via copulas: theoretical aspects and applications to  
609 hydrological events. *Water Resour Res* 40(12): 229–244
- 610 Schulte M, Schumann AH (2016) Evaluation of flood coincidence and retention measures by copulas.  
611 *Wasserwirtschaft* 106(2–3): 81–87
- 612 Schweizer B, Sklar A (1983) Probabilistic metric spaces. Elsevier Science, New York
- 613 Shiau JT (2006) Fitting drought and severity with two-dimensional copulas. *Water Resour Manag* 20(5):  
614 795- 815
- 615 Shimizu K (2010) A bivariate mixed Lognormal distribution with an analysis of rainfall data. *J Appl*  
616 *Meteorol Clim* 32(2): 161-171
- 617 Silverman BW (1986) Density Estimation for Statistics and Data Analysis. Chapman and Hall, New York

- 618 Sraj M, Bezak N, Brilly M (2015) Bivariate flood frequency analysis using the copula function: a case  
619 study of the Litija station on the Sava River. *Hydrol Process* 29: 235–248.  
620 <https://doi.org/10.1002/hyp.10145>
- 621 Thielen AH, Apel H, Merz B (2015) Assessing the probability of large-scale flood loss events: a case  
622 study for the river Rhine, Germany. *J Flood Risk Manag* 8: 247-262.  
623 <https://doi.org/10.1111/jfr3.12091>
- 624 Wang B, Xiang BQ, Lee JY (2013) Subtropical high predictability establishes a promising way for  
625 monsoon and tropical storm predictions. *P Natl Acad Sci USA* 110(8): 2718-2722
- 626 Wang C (2016) A joint probability approach for coincidental flood frequency analysis at ungauged basin  
627 confluences. *Nat Hazards* 82(3): 1727-1741. <https://doi.org/10.1007/s11069-016-2265-5>
- 628 Wang C, Chang NB, Yeh GT (2009) Copula-based flood frequency (COFF) analysis at the confluences of  
629 river systems. *Hydrol Process* 23(10): 1471–1486. <https://doi.org/10.1002/hyp.7273>
- 630 Weiss MS (1978) Modification of the Kolmogorov–Smirnov statistic for use with correlated data. *J Am*  
631 *Stat Assoc* 73(364): 872–875
- 632 Xiao Y, Guo SL, Liu P et al (2009) Design flood hydrograph based on multi-characteristic synthesis index  
633 method. *J Hydrol Eng* 14(12): 1359–1364. [https://doi.org/10.1061/\(ASCE\)1084-  
634 0699\(2009\)14:12\(1359\)](https://doi.org/10.1061/(ASCE)1084-0699(2009)14:12(1359))
- 635 Xiong F, Guo SL, Liu P et al (2019) A general framework of design flood estimation for cascade reservoirs  
636 in operation period. *J Hydrol* 577: 124003
- 637 Yin JB, Guo SL, Liu ZJ et al (2018) Uncertainty analysis of bivariate design flood estimation and its  
638 impacts on reservoir routing. *Water Resour Manag* 32(5): 1795-1809
- 639 Yue S (1999) Applying the bivariate normal distribution to flood frequency analysis. *Water Int* 24(3): 248–  
640 254. <https://doi.org/10.1080/02508069908692168>
- 641 Yue S (2000a) The bivariate lognormal distribution to model a multivariate flood episode. *Hydrol Process*

642 14 (14): 2575- 2588

643 Yue S (2000b) Joint probability distribution of annual maximum storm peaks and amounts as represented  
644 by daily rainfalls. *Hydrol Sci J* 45(2): 315-326

645 Yue S (2002) The bivariate lognormal distribution for describing joint statistical properties of a  
646 multivariate storm event. *Environmetrics* 13: 811-819

647 Zhang L, Singh VP (2006) Bivariate flood frequency analysis using the copula method. *J Hydrol Eng*  
648 11(2): 150–164. [https://doi.org/10.1061/\(ASCE\)1084-0699\(2006\)11:2\(150\)](https://doi.org/10.1061/(ASCE)1084-0699(2006)11:2(150))

649 Zhang L, Singh VP (2007) Trivariate flood frequency analysis using the Gumbel-Hougaard copula. *J*  
650 *Hydrol Eng* 12(4): 431–439. [https://doi.org/10.1061/\(ASCE\)1084-0699\(2007\)12:4\(431\)](https://doi.org/10.1061/(ASCE)1084-0699(2007)12:4(431))

651 Zhang L, Singh VP (2012) Bivariate rainfall and runoff analysis using entropy and copula theories. *Entropy*  
652 14(9): 1784–1812. <https://doi.org/10.3390/e14091784>.

653 Zhang WJ, Jin F, Stuecker MF et al (2016) Unraveling El Niño's impact on the East Asian Monsoon and  
654 Yangtze River summer flooding. *Geophys Res Lett* 43: 11375–  
655 11382. <https://doi.org/10.1002/2016GL071190>

656 Zhong YX, Guo SL, Liu ZJ et al (2018) Quantifying differences between reservoir inflows and dam site  
657 floods using frequency and risk analysis methods. *Stoch Environ Res Risk Assess* 32(2): 419-433

658

659 Lists of Tables

660 **Table 1** Parameters and test results of marginal distributions of flood occurrence dates

661 **Table 2** Parameters and test results of marginal distributions of flood magnitudes

662 **Table 3** Parameters and test results of joint distributions of flood occurrence dates and magnitudes

663 **Table 4** Joint probabilities and co-occurrence probabilities of flood magnitudes at Liaojiawan and Loujiacun stations

664 (%)

665 **Table 5** Conditional probabilities of flood magnitudes at three stations (%)

666 **Table 6** Statistical analysis of design floods at three stations in Fuhe River

667 **Table 7** Comparative analysis of flood coincidence probabilities under different conditions

668 **Table 1** Parameters and test results of marginal distributions of flood occurrence dates

Station	$u_i$	$k_i$	$p_i$	K-S	RMSE
Liaojiawan	1.82	6.11	0.13	0.061(0.167)	0.022
	2.28	39.34	0.14		
	2.98	10.86	0.73		
Loujiacun	2.58	3.01	0.68	0.053(0.167)	0.019
	2.98	32.51	0.32		
	2.75	8.04	0.00		
Lijiadu	1.83	1.75	0.15	0.085(0.167)	0.033
	2.82	8.98	0.54		
	2.96	3.42	0.31		

669



670 **Table 2** Parameters and test results of marginal distributions of flood magnitudes

Station	Mean (m <sup>3</sup> /s)	<i>C<sub>v</sub></i>	<i>C<sub>s</sub></i>	<i>p</i> -value ( $\chi^2$ )	RMSE
Liaojiawan	2861.69	0.51	0.77	0.249 (0.05)	0.047
Loujiacun	1903.75	0.43	0.78	0.249 (0.05)	0.025
Lijiadu	4570.62	0.45	0.63	0.247 (0.05)	0.055

671

672 **Table 3** Parameters and test results of joint distributions of flood occurrence dates and magnitudes

Joint distribution	Clayton		GH		Frank	
	$\theta$	RMSE	$\theta$	RMSE	$\theta$	RMSE
Occurrence dates between Liaojiawan and Loujiacun	3.69	0.028	2.84	0.030	9.38	0.029
Flood magnitudes between Liaojiawan and Loujiacun	2.59	0.033	2.30	0.043	7.05	0.037
Flood magnitudes between Liaojiawan and Lijiadu	6.25	0.039	4.12	0.048	14.64	0.043
Flood magnitudes between Loujiacun and Lijiadu	4.99	0.034	3.49	0.045	12.07	0.041

673

674 **Table 4** Joint probabilities and co-occurrence probabilities of flood magnitudes at Liaojiawan and Loujiacun stations  
 675 (%)

Station	Loujiacun						Coincidence probabilities
	T (year)	5	10	20	50	100	
Liaojiawan	5	30.48	24.85	22.33	20.91	20.45	Joint probabilities
	10	24.85	17.14	13.50	11.38	10.69	
	20	22.33	13.50	9.20	6.67	5.83	
	50	20.91	11.38	6.67	3.86	2.93	
	100	20.45	10.69	5.83	2.93	1.96	
	5	9.52	5.15	2.67	1.09	0.55	Co-occurrence probabilities
	10	5.15	2.86	1.50	0.62	0.31	
	20	2.67	1.50	0.80	0.33	0.17	
	50	1.09	0.62	0.33	0.14	0.07	
	100	0.55	0.31	0.17	0.07	0.04	

676

677 **Table 5** Conditional probabilities of flood magnitudes at three stations (%)

Station	Lijiadu					
	T (year)	5	10	20	50	100
Liaojiawan	5	16.41	9.23	4.83	1.98	0.99
	10	8.20	5.01	2.74	1.15	0.58
	20	4.06	2.59	1.46	0.62	0.32
	50	1.61	1.06	0.61	0.26	0.14
	100	0.80	0.53	0.31	0.13	0.07
Loujiacun	5	15.21	8.48	4.43	1.82	0.91
	10	7.54	4.47	2.42	1.01	0.51
	20	3.73	2.29	1.26	0.54	0.27
	50	1.48	0.93	0.52	0.22	0.11
	100	0.74	0.47	0.26	0.11	0.06

678

679 **Table 6** Statistical analysis of design floods at three stations in Fuhe River

Return period (year)	5	10	20	50	100
Design flood at Liaojiawan (m <sup>3</sup> /s)	4007	4816	5543	6430	7061
Design flood at Loujiacun (m <sup>3</sup> /s)	2544	2997	3406	3904	4258
Simulated flood at Lijiadu (m <sup>3</sup> /s)	6227	7397	8451	9735	10649
Simulated flood frequency at Lijiadu (%)	19.79	9.41	4.41	1.59	0.73
Return period at Lijiadu (year)	5	11	23	63	137

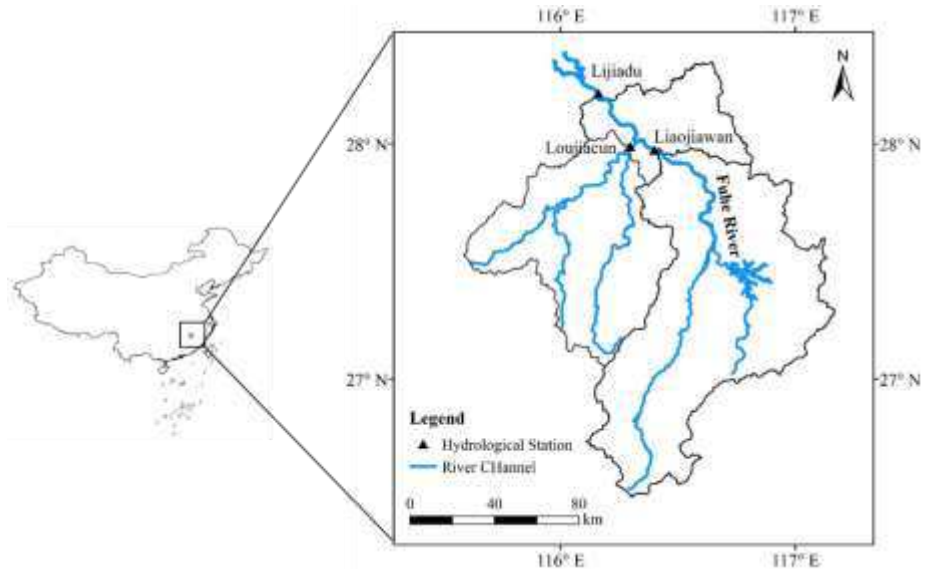
680

681 **Table 7** Comparative analysis of flood coincidence probabilities under different conditions

Return period (year)	5	10	20	50	100
Simulated flood frequency (%)	19.79	9.41	4.41	1.59	0.73
Joint probability (%)	30.48	17.14	9.20	3.86	1.96
Co-occurrence probability (%)	9.52	2.86	0.80	0.14	0.04
Conditional probability $P_1^c$ (%)	16.41	5.01	1.46	0.26	0.07
Conditional probability $P_2^c$ (%)	15.21	4.47	1.26	0.22	0.06

682

683	Lists of Figures
684	<b>Fig. 1</b> Location of hydrological stations in the Fuhe River basin
685	<b>Fig. 2</b> Correlation analysis of annual maximum flood variables in Fuhe River
686	<b>Fig. 3</b> Multiple regression model fitting results of flood variables at Lijiadu station
687	<b>Fig. 4</b> Fitted empirical and theoretical probabilities of marginal distributions
688	<b>Fig. 5</b> Fitted empirical and theoretical probabilities of joint distributions
689	<b>Fig. 6</b> Daily coincidence probabilities of occurrence dates of annual maximum flood at Liaojiawan and Loujiacun
690	stations
691	<b>Fig. 7</b> Flood coincidence probabilities under different conditions
692	

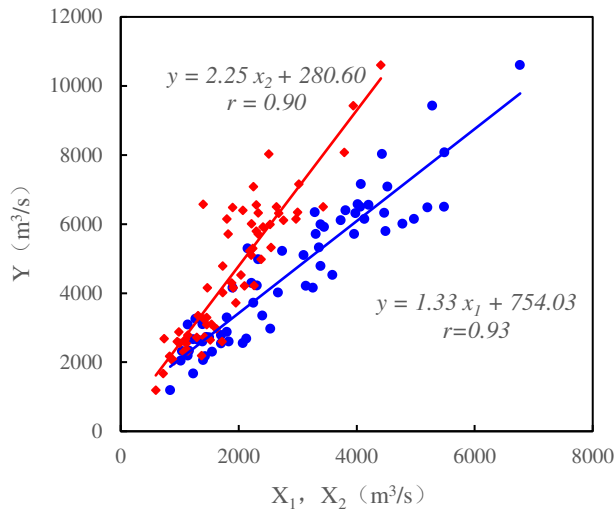


693

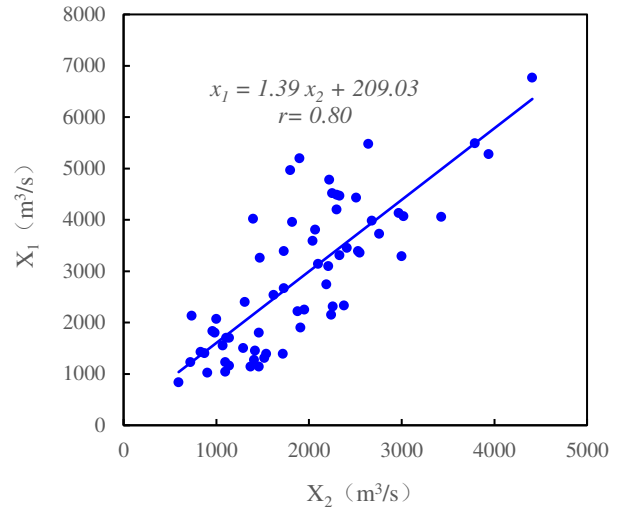
694

**Fig. 1** Location of hydrological stations in the Fuhe River basin



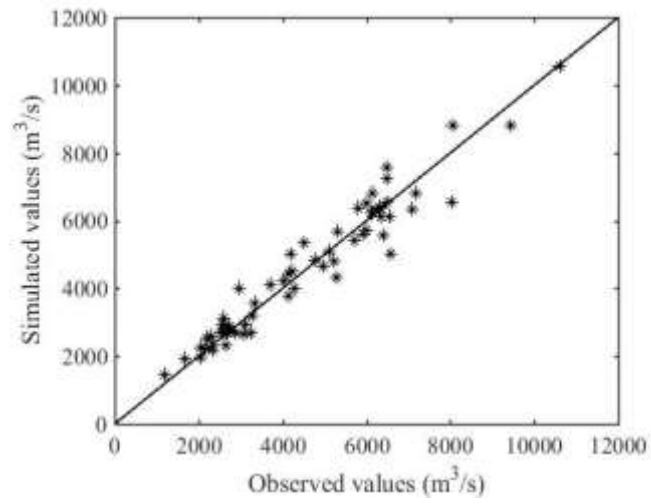


(a)  $Y \sim X_1$  and  $Y : X_2$



(b)  $X_1 \sim X_2$

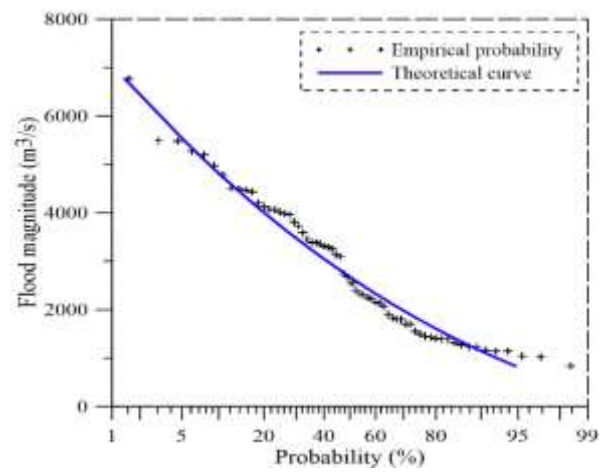
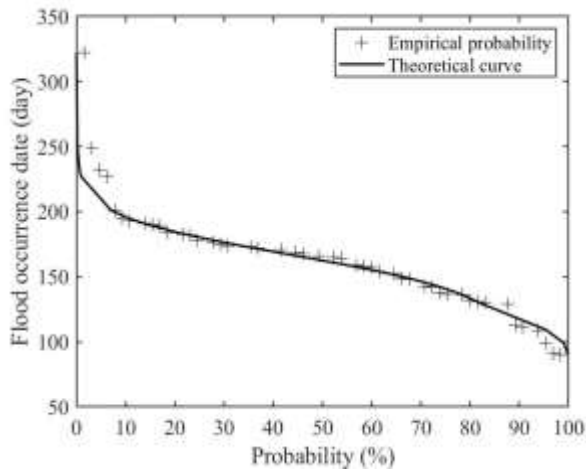
695 **Fig. 2** Correlation analysis of annual maximum flood variables in Fuhe River



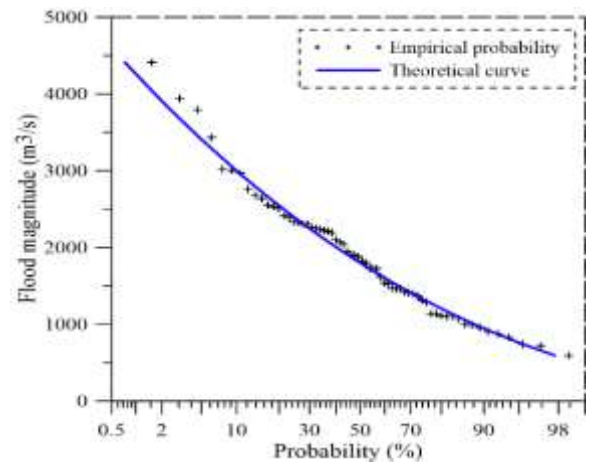
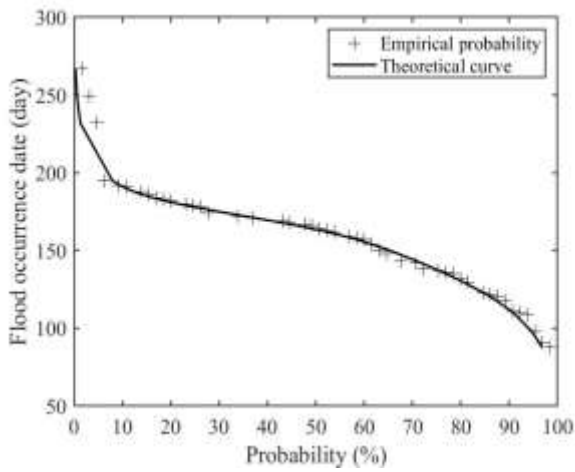
696

697

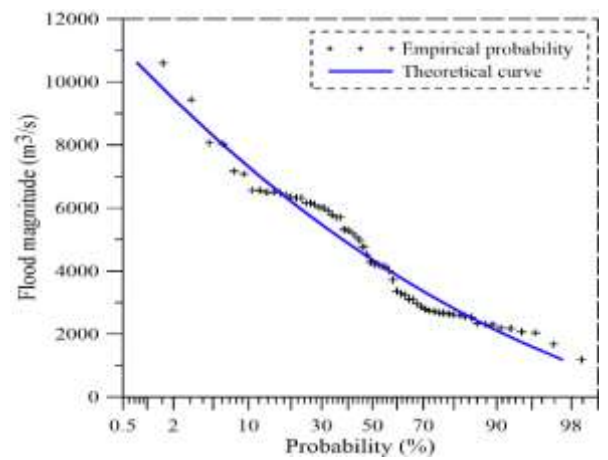
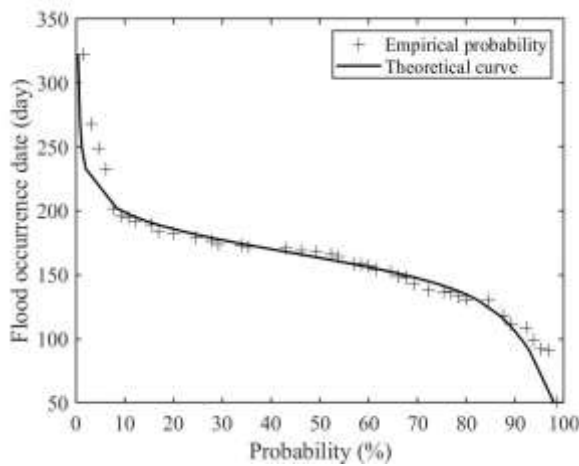
**Fig. 3** Multiple regression model fitting results of flood variables at Lijiadu station



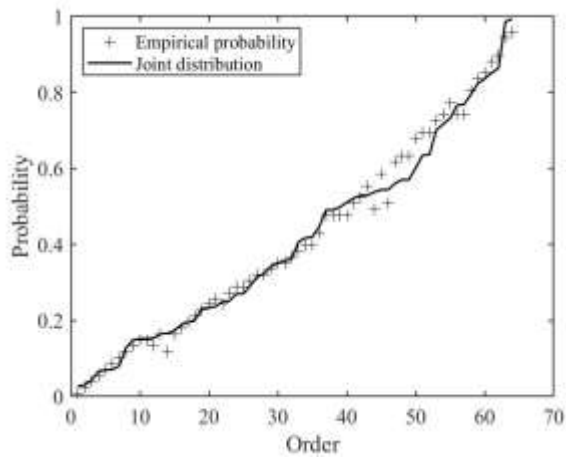
(a) Flood occurrence dates and flood magnitudes at Liaojiawan station



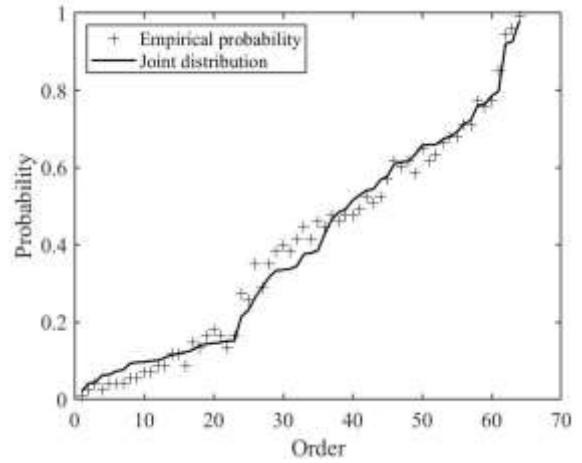
(b) Flood occurrence dates and flood magnitudes at Loujiacun station



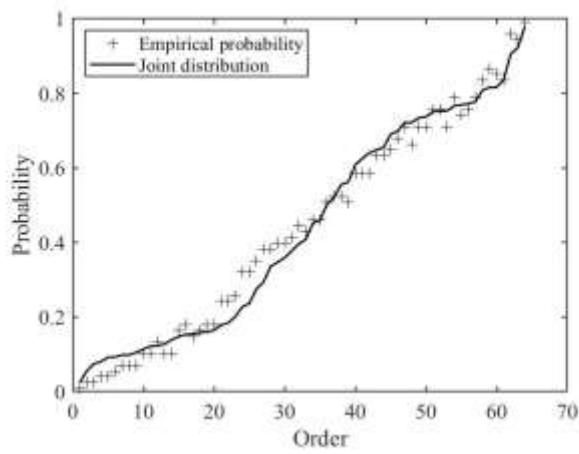
(c) Flood occurrence dates and flood magnitudes at Lijiadu station



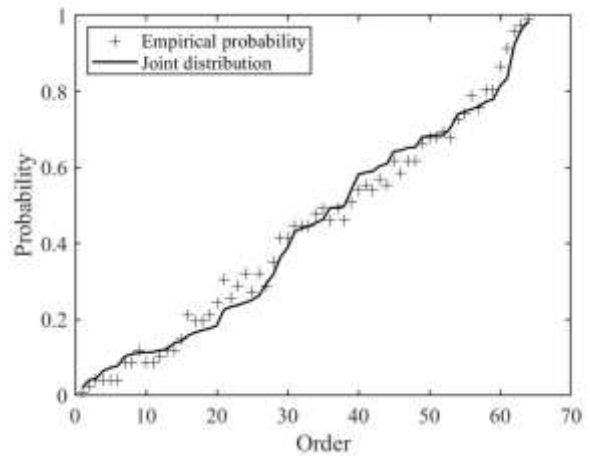
(a) Occurrence dates between Liaojiawan and Loujiacun stations



(b) Flood magnitudes between Liaojiawan and Loujiacun stations

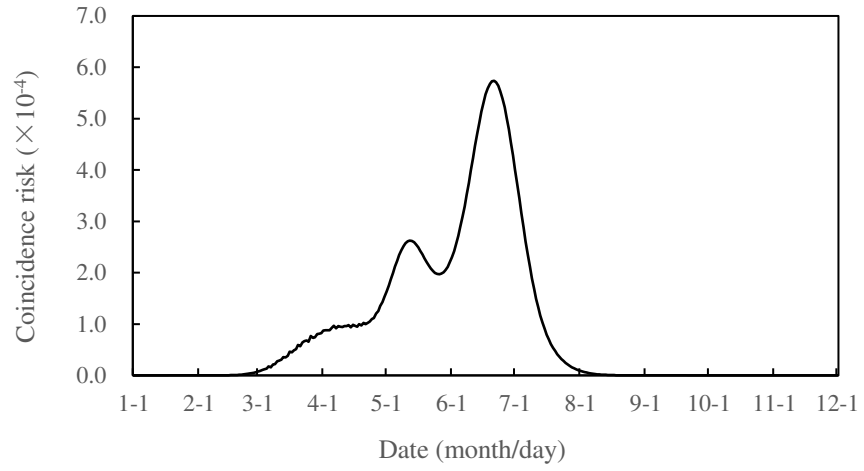


(c) Flood magnitudes between Liaojiawan and Lijiadu stations



(d) Flood magnitudes between Loujiacun and Lijiadu stations

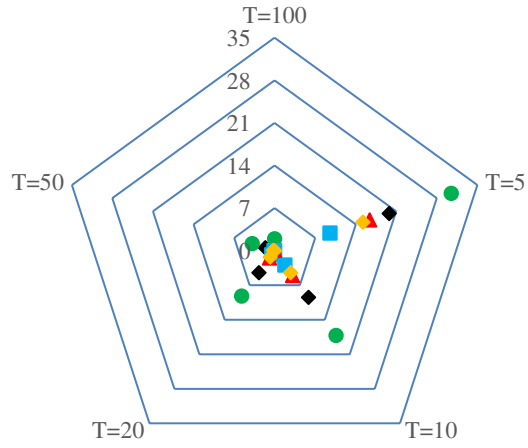
699 **Fig. 5** Fitted empirical and theoretical probabilities of joint distributions



700

701 **Fig. 6** Daily coincidence probabilities of occurrence dates of annual maximum flood at Liaojiawan and Loujiacun

702 stations



- ◆ Simulated flood frequency
- Joint probability
- Co-occurrence probability
- ▲ Conditional probability Pc1
- ◆ Conditional probability Pc2 (%)

703

704

705

**Fig. 7** Flood coincidence probabilities under different conditions